



Supplement of

Terrestrial runoff is an important source of biological ice-nucleating particles in Arctic marine systems

Corina Wieber et al.

Correspondence to: Tina Šantl-Temkiv (temkiv@bio.au.dk)

The copyright of individual parts of the supplement might differ from the article licence.

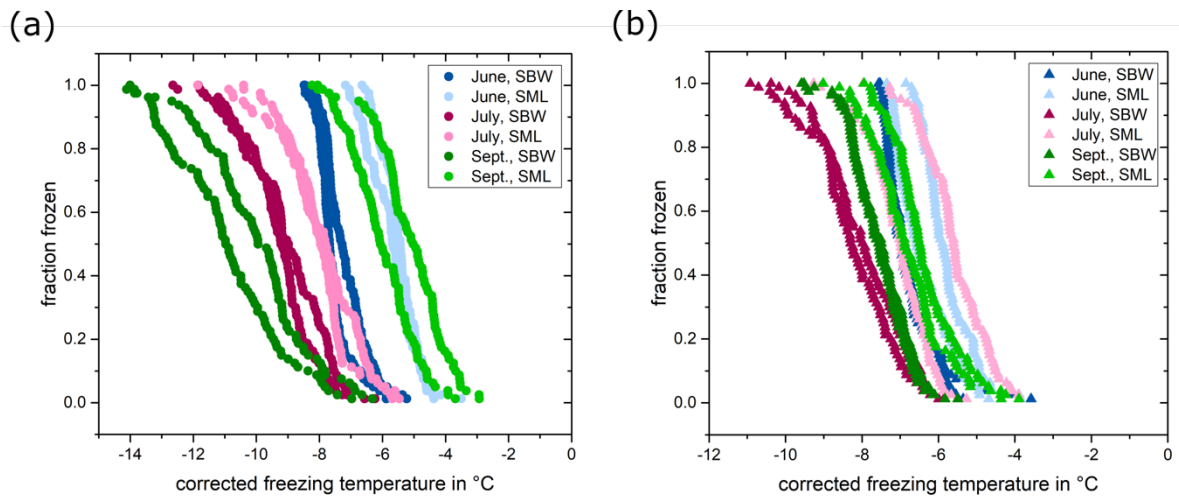


Figure S1: Fraction frozen curves for the undiluted samples for the Kobbefjord (a) and the Godthåbsfjord (b). All samples are analyzed in duplicates.

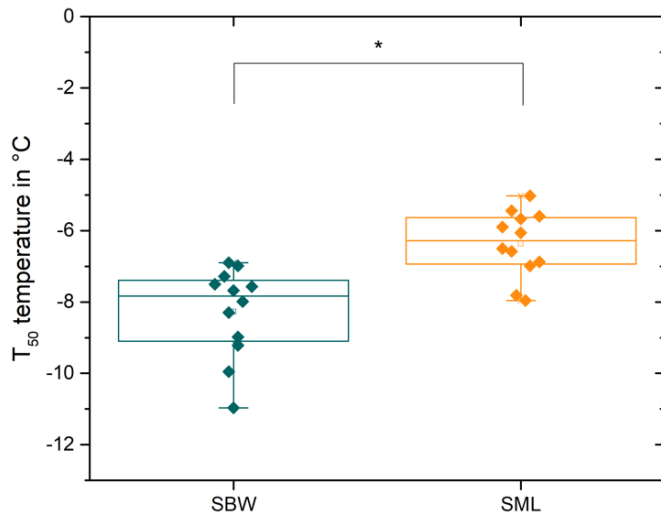


Figure S2: T_{50} temperatures for the SBW samples in comparison to the SML samples shown as box plot with 25th and 75th percentiles. T_{50} temperatures are significantly higher in the SML (Mann-Whitney test, $p < 0.01$).

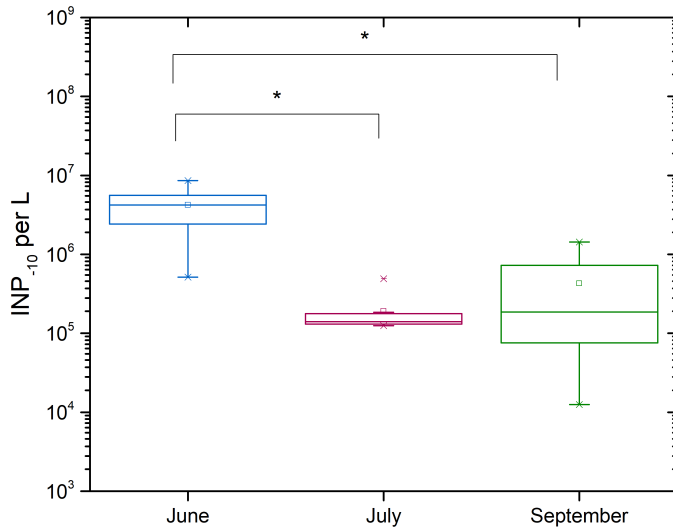


Figure S3: Concentration of INPs active at -10 °C for SBW and SML samples separated by months shown as box plot with 25th and 75th percentiles. INP₋₁₀ concentrations are significantly higher in June compared to July (Mann-Whitney test, $p < 0.01$) and September (Mann-Whitney test, $p = 0.01$).

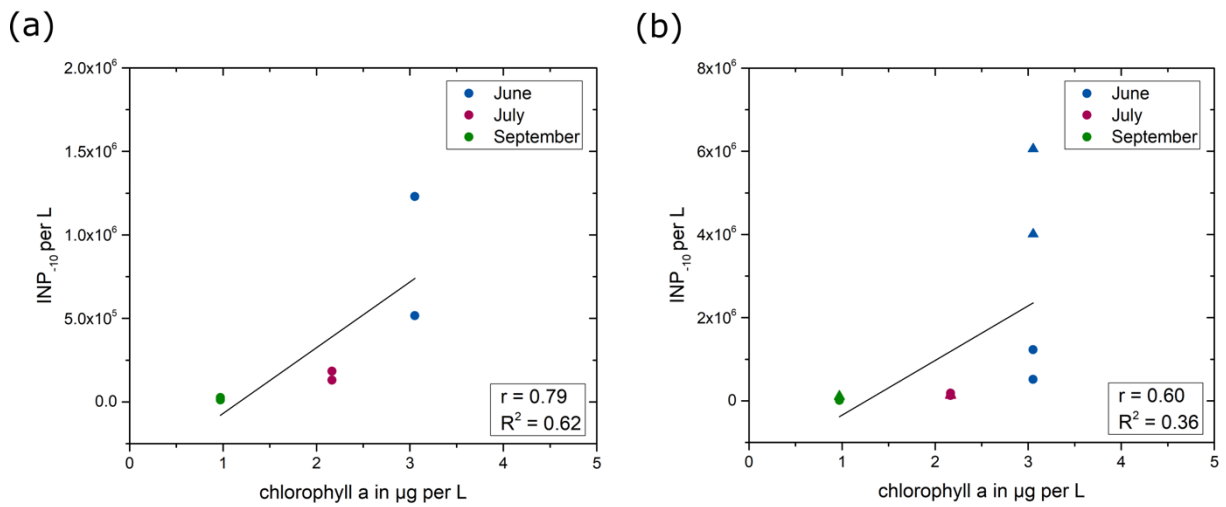


Figure S4: Number of INPs active at -10 °C in relation to the chlorophyll concentration measured on the sampling dates at Kobbefjord. (a) only data for SBW samples from Kobbefjord ($p = 0.064$), (b) data from SBW samples in Kobbefjord (circles) and Godthåbsfjord (triangles) ($p = 0.038$).

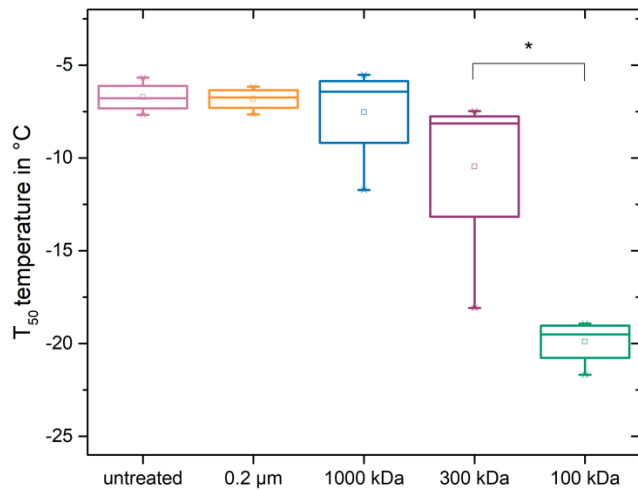


Figure S5: T₅₀ temperatures for the June samples (each box contains SBW and SML samples (n = 4)) after filtration treatments shown as box plot with 25th and 75th percentiles. T₅₀ temperatures after filtration with 100 kDa are significantly lower (Mann-Whitney test, p < 0.05). For illustrative purposes only significance between the 300 kDa and 100 kDa samples is indicated in the figure.

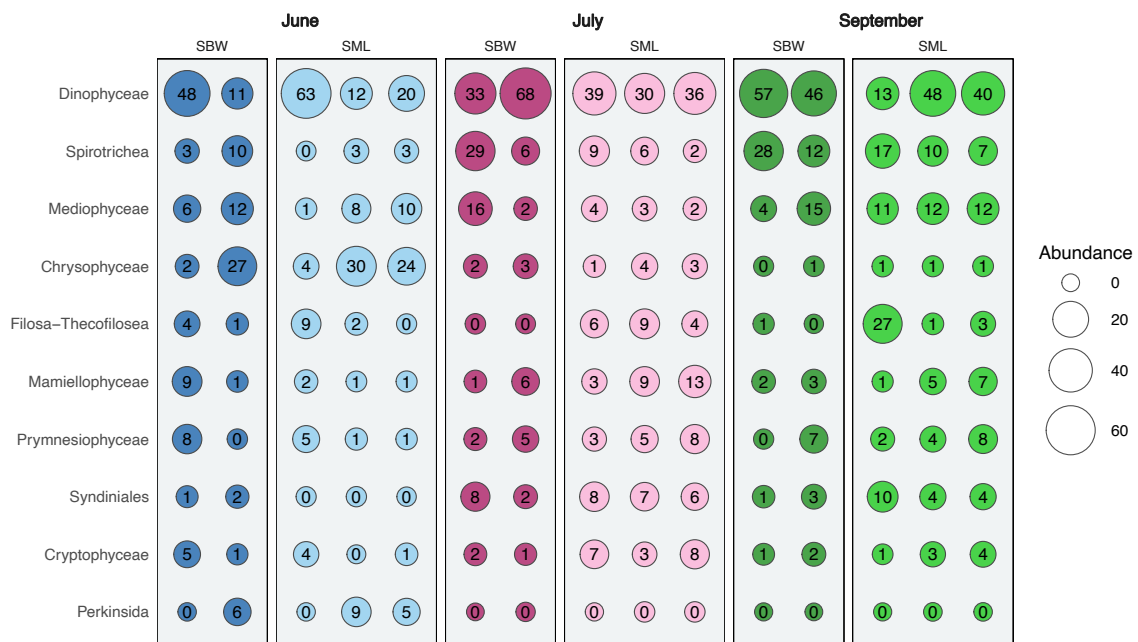


Figure S6: Eukaryotic community composition derived from the 18S rRNA data on the class level. The abundance is indicated by the size of the circle and given in percent rounded to the closest whole number inside the circles.

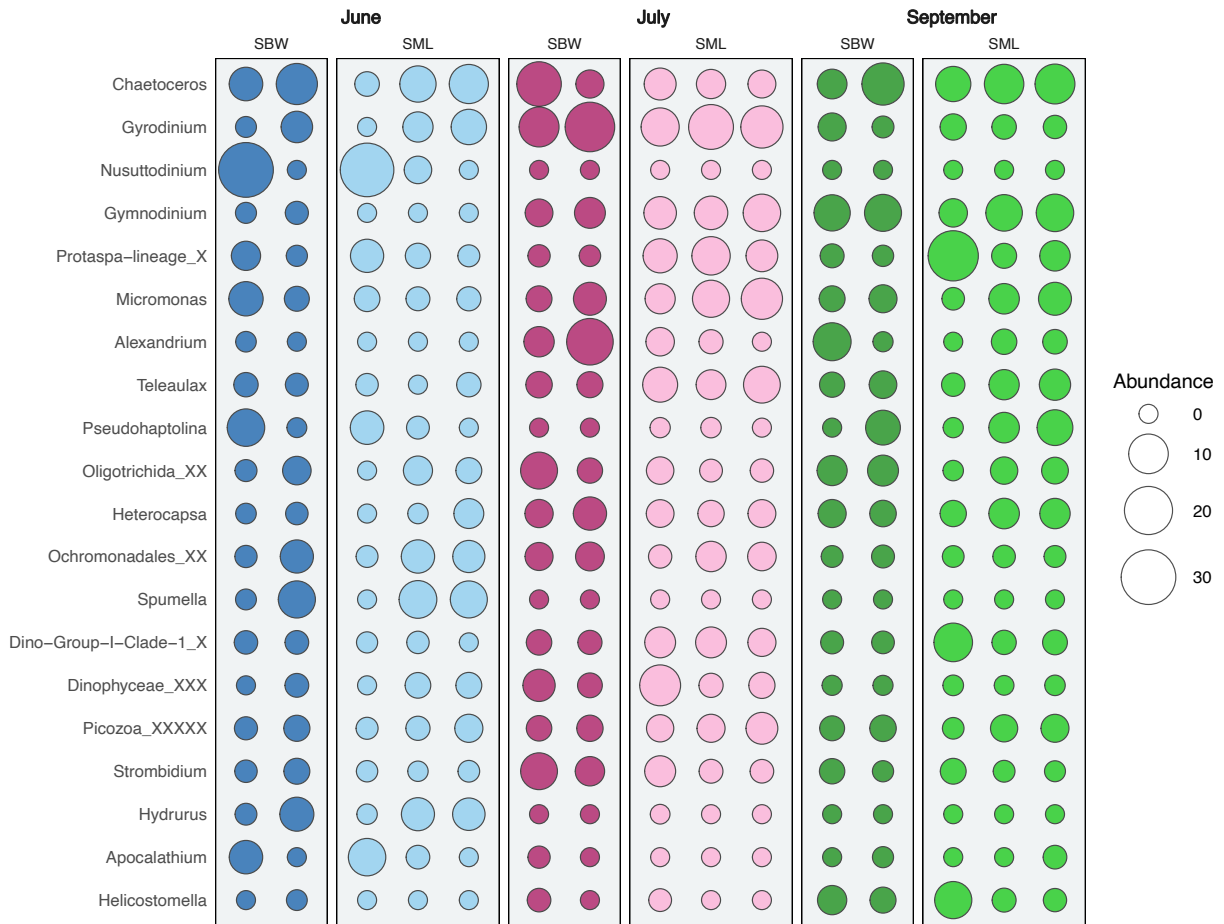


Figure S7: Eukaryotic community composition derived from the 18S rRNA data on the genus level. The abundance is indicated by the size of the circle.

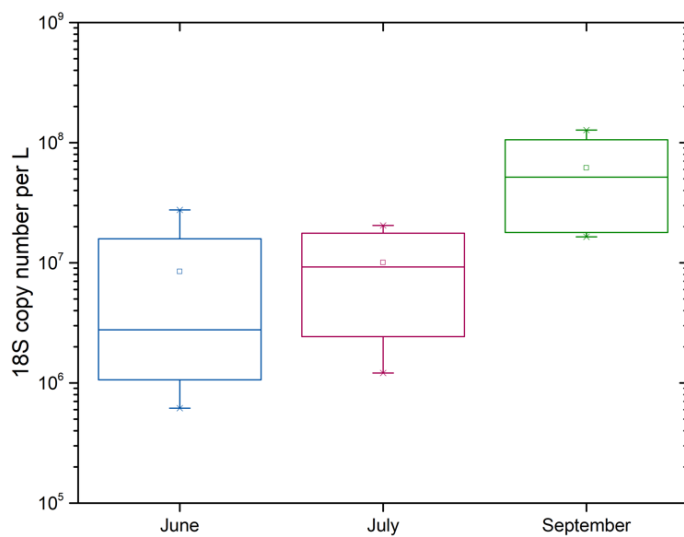


Figure S8: Ribosomal gene copy numbers based on the 18S rRNA data. Differences in copy numbers are not significant (Kruskal-Wallis, $p = 0.123$).

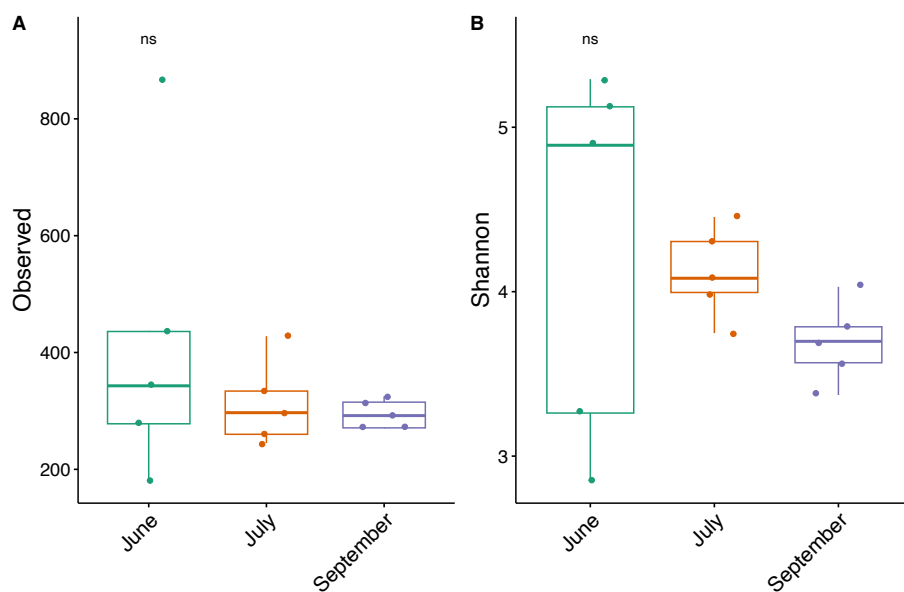


Figure S9: Observed and Shannon diversity for the 18S rRNA data. No significant differences are observed in this datasets (Mann-Whitney test, $p > 0.05$).

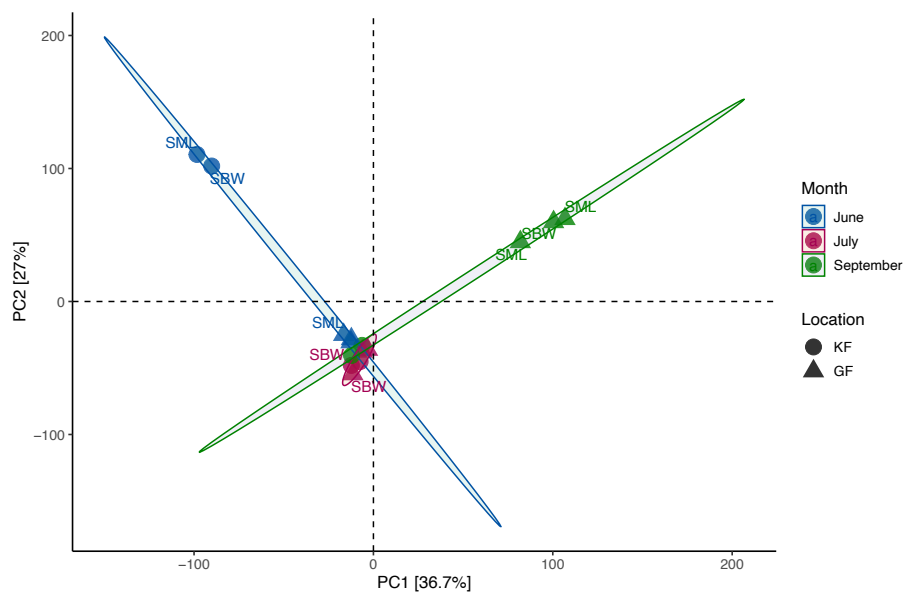


Figure S10: Principal component analysis for the eukaryotic community (18S rRNA). PC1 emerges as the most influential, encapsulating 36.7% of the total variance. Followed by PC2 (27%) collectively representing a significant portion of the compositional diversity.

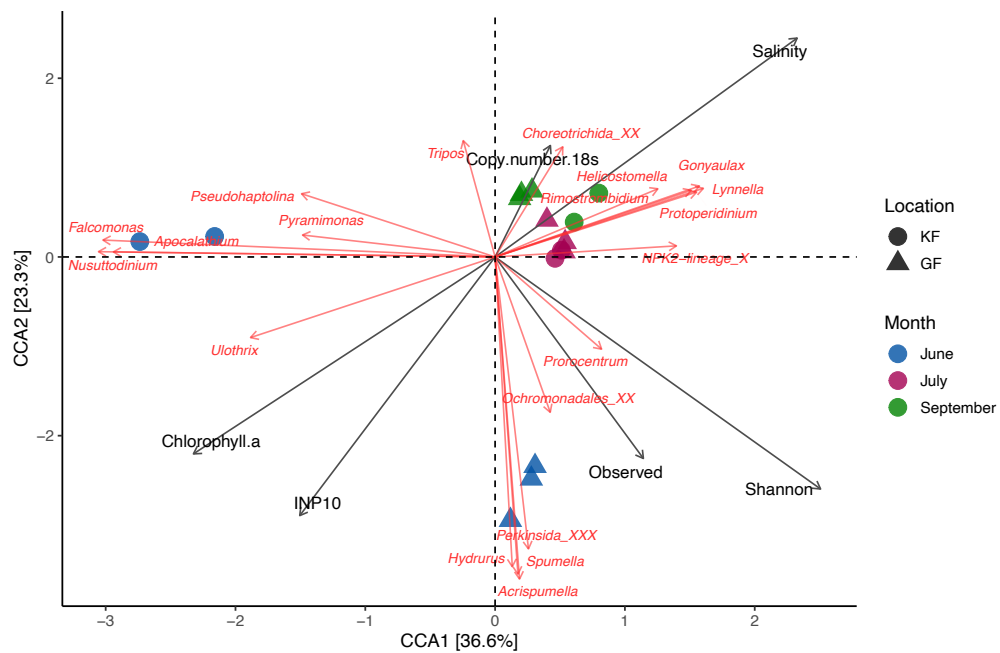


Figure S11: Canonical correspondence analysis for the 18S rRNA data (20 taxa). The total inertia in the dataset was 2.7093, partitioned into constrained and unconstrained inertias. Constrained inertia accounted for a substantial proportion (63.85%) of the total inertia.

Table S1: Mantel test for the 18S rRNA data using the robust Aitchison distance. The results indicated significant correlation for salinity, chlorophyll a and Shannon diversity while all other variables showed no correlation ($p > 0.05$).

Variable	Correlation Coefficient	p-value	Significance
18S copy number	0.100	0.279	-
INP ₋₁₀	0.149	0.166	-
Salinity	0.376	0.004	*
Chlorophyll a	0.388	0.001	**
Observed alpha diversity	0.332	0.043	-
Shannon index	0.330	0.010	*

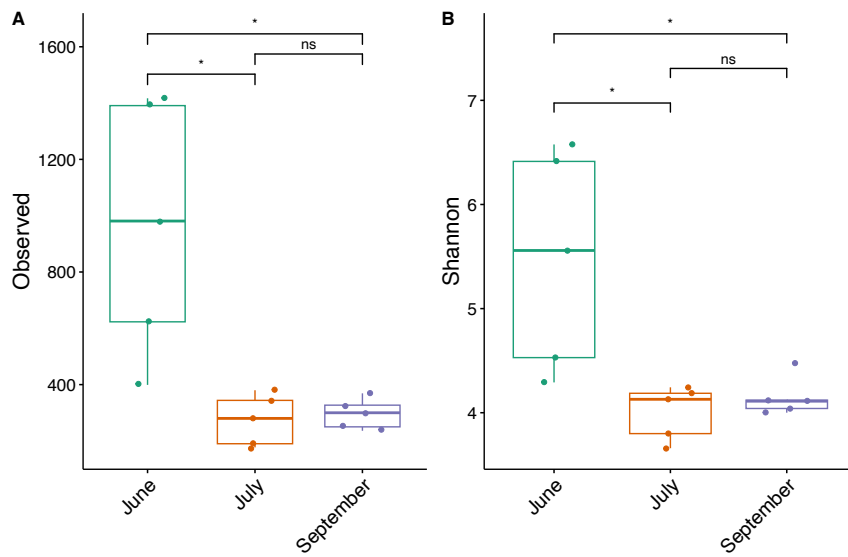


Figure S12: Observed and Shannon diversity for the 16S rRNA data. Significance is indicated by an asterisk, n.s. stands for not significant (Mann-Whitney test). The Observed diversity is significantly higher in June compared to July ($p = 0.024$) and compared to September ($p = 0.024$). The Shannon diversity follows the same pattern with p -values of 0.024 and 0.043, respectively.

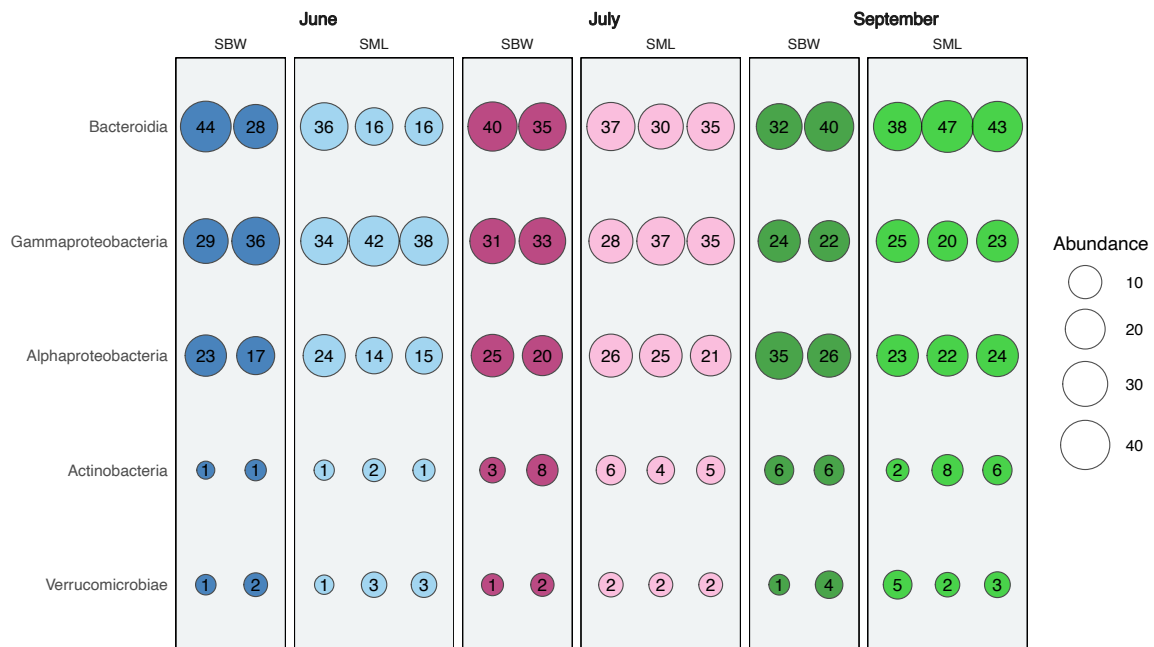


Figure S13: Bacterial community composition derived from the 16S rRNA data on the class level. The abundance is indicated by the size of the circle and given in percent rounded to the closest whole number inside the circles.

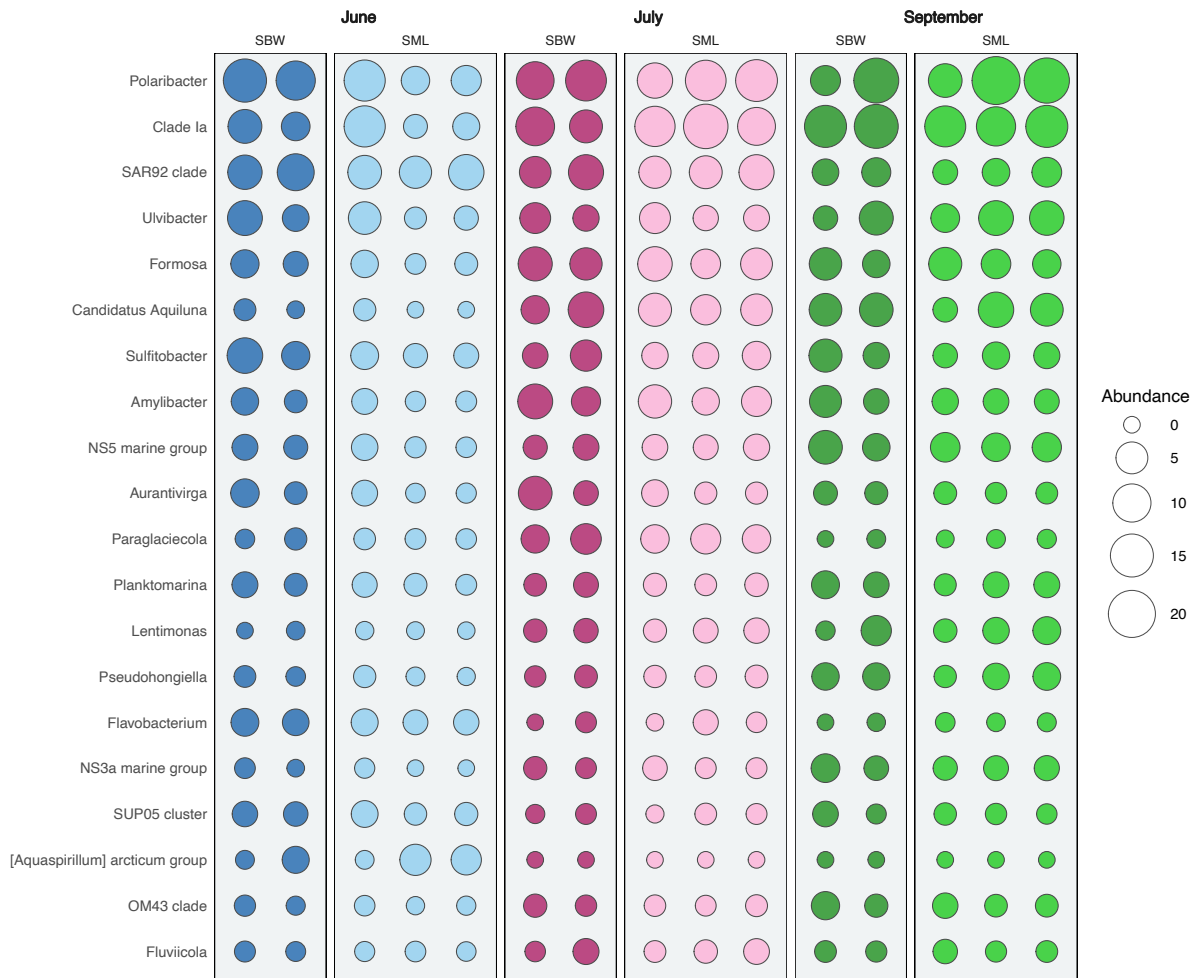


Figure S14: Bacterial community composition derived from the 16S rRNA data on the genus level. The abundance is indicated by the size of the circle.

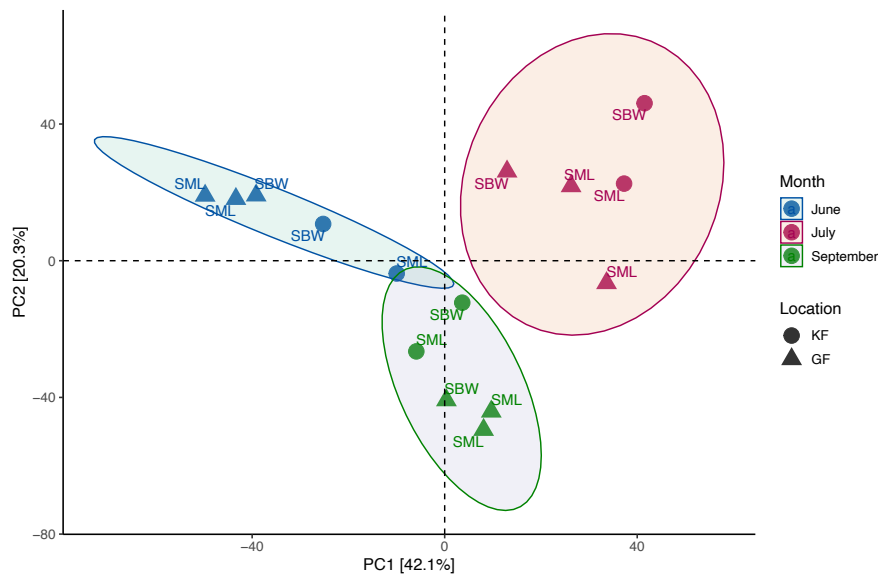


Figure S15: Principal component analysis for the bacterial community. Eigenvalues from PCA revealed that the first few principal components (PC1-PC3) contribute significantly to the variance in the bacterial community composition. PC1 was the most influential, representing 42.1% of the total variance, followed by PC2 (20.3%) and PC3 (12.6%).

Table S2: Mantel test to assess the correlation between bacterial community dissimilarities (measured using robust Aitchison distance) and environmental parameters.

Variable	Correlation Coefficient	p-value	Significance
16S copy number	0.184	0.130	-
INP ₋₁₀	0.650	0.003	**
Salinity	0.670	0.003	**
Chlorophyll a	0.311	0.010	**
Observed alpha diversity	0.640	0.003	**
Shannon index	0.650	0.003	**

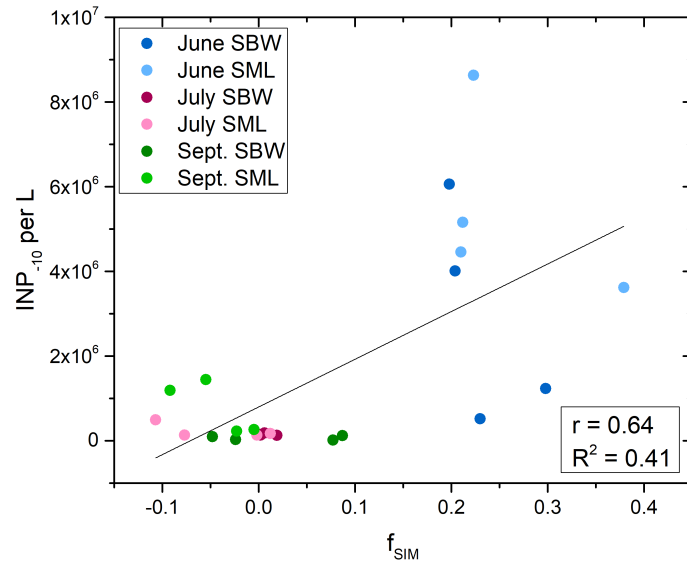


Figure S16: Correlation between the freshwater fraction of sea ice melt and the number of INPs active at -10 °C. The line represents a linear regression for all data points ($p < 0.001$).